

Closing in on t -channel simplified dark matter models

Chiara Arina^a, Benjamin Fuks^{b,c}, Luca Mantani^a, Hanna Mies^d, Luca Panizzi^{e,f} and Jakub Salko^e

^aCentre for Cosmology, Particle Physics and Phenomenology (CP3), Université catholique de Louvain, B-1348 Louvain-la-Neuve, Belgium

^bSorbonne Université, CNRS, Laboratoire de Physique Théorique et Hautes Énergies, LPTHE, F-75005 Paris, France

^cInstitut Universitaire de France, 103 boulevard Saint-Michel, F-75005 Paris, France

^dInstitute for Theoretical Particle Physics and Cosmology, RWTH Aachen University, D-52056 Aachen, Germany

^eDepartment of Physics and Astronomy, Uppsala University, Box 516, SE-751 20 Uppsala, Sweden

^fSchool of Physics and Astronomy, University of Southampton, Highfield, Southampton SO17 1BJ, UK

ARTICLE INFO

Keywords:

Dark matter simplified models, collider searches, cosmological bounds

ABSTRACT

A comprehensive analysis of cosmological and collider constraints is presented for three simplified models characterised by a dark matter candidate (real scalar, Majorana fermion and real vector) and a coloured mediator (fermion, scalar and fermion respectively) interacting with the right-handed up quark of the Standard Model. Constraints from dark matter direct and indirect detection and relic density are combined with bounds originating from the re-interpretation of a full LHC run 2 ATLAS search targeting final states with multiple jets and missing transverse energy. Projections for the high-luminosity phase of the LHC are also provided to assess future exclusion and discovery reaches, which show that analogous future search strategies will not allow for a significant improvement compared with the present status. From the cosmological point of view, we demonstrate that thermal dark matter is largely probed (and disfavoured) by constraints from current direct and indirect detection experiments. These bounds and their future projections have moreover the potential of probing the whole parameter space when combined with the expectation of the high-luminosity phase of the LHC.

1. Introduction

The nature of dark matter and the way it is connected to the Standard Model (SM) is one of the most puzzling issues in particle physics today. Dark matter searches consequently hold a central place in the present astroparticle and particle physics program. However, despite of convincing indirect evidence for its existence [1], dark matter still evades any direct detection probes. Experimental searches at colliders, in underground nuclear recoil experiments and with gamma-ray telescopes therefore put stronger and stronger constraints on the viability of any dark matter model. Those bounds are very often explored, in a model-independent approach, as limits on a set of simplified models for dark matter phenomenology. In those simplified models, the dark matter is considered as a massive particle whose interactions with the SM arise through a mediator particle. In so-called s -channel setups [2, 3, 4], the mediator is a colour singlet and couples to a pair of either dark matter or SM particles. On the contrary, in a t -channel configuration, the mediator interacts instead with one SM state and the dark matter [5].

In this work, we consider three simplified t -channel scenarios, that we coin F3S_{uR}, S3M_{uR} and F3V_{uR}, and that are defined in ref. [5]. Their common features are the following. First, the dark matter candidate is a real particle, singlet under the SM gauge group, so that its stability can be ensured through a \mathbb{Z}_2 symmetry. This contrasts with other t -channel models including a complex dark matter field and thus exhibiting instead a continuous unbroken global $U(1)$ symmetry. Second, the mediator couples the dark matter candidate to the right-handed up-quark field, so that the mediator is itself an $SU(2)_L$ weak singlet. Other choices are however

possible, as dark matter could interact with different quark flavours and chiralities. The u_R choice is only one of the numerous possibilities, justified by its simplicity (it only involves weak singlets) and by the enhancement of the relevant collider and direct detection processes due to valence quarks. We will nevertheless highlight, in the following, wherever other mediator choices could make a difference. The defining features of the three scenarios then consist in the spins of the dark matter and of the mediator, which affect the kinematics of any signal and therefore current bounds and projections for future searches. We comprehensively derive updated constraints on the three model parameter spaces, considering both cosmological and collider observations. Moreover, we additionally provide projections for the future high-luminosity phase of the LHC (HL-LHC).

The rest of the paper is organised as follows. In the next section we briefly define the DMSimpt general framework for t -channel dark matter models, while in section 3 we describe our analysis of the collider constraints and provide results with current exclusion bounds. In section 4 we study the astrophysical and cosmological constraints on these simplified models under the assumption of thermal relic dark matter. In section 5 we combine these results and include future experiment expectations, illustrating the impact of the collider/cosmology combination on representative projections of the model parameter space. We summarise our main findings and discuss future developments in section 6.

2. The t -channel simplified models

The three simplified models under study are defined within the DMSimpt framework [5], which provides a generic t -channel dark matter simplified model. In the latter, the SM

ORCID(s):

is extended by six real or complex dark matter fields, collectively denoted by X and all singlets under the SM gauge group $SU(3)_c \times SU(2)_L \times U(1)_Y$, plus the corresponding mediator particles, collectively denoted by Y , all lying in the fundamental representation of $SU(3)_c$ and coupling the X particles to the SM quarks.

The scenarios considered in the present analysis are restrictions of the general DMSimpt framework to setups in which the dark matter particle X is real and solely couples to the right-handed up-quark. There is hence a unique mediator particle Y , singlet under $SU(2)_L$. The corresponding interaction Lagrangians for the F3S_uR (real scalar dark matter \tilde{S} with a fermionic mediator ψ), S3M_uR (Majorana dark matter $\tilde{\chi}$ with a scalar mediator ϕ) and F3V_uR (real vector dark matter \tilde{V}_μ with a fermionic mediator ψ) models respectively read

$$\begin{aligned}\mathcal{L}_{\text{F3S_uR}} &= \left[\hat{\lambda}_\psi \bar{\psi} u_R \tilde{S} + \text{h.c.} \right], \\ \mathcal{L}_{\text{S3M_uR}} &= \left[\lambda_\phi \tilde{\chi} u_R \phi^\dagger + \text{h.c.} \right], \\ \mathcal{L}_{\text{F3V_uR}} &= \left[\hat{\lambda}_\psi \bar{\psi} \tilde{V} u_R + \text{h.c.} \right].\end{aligned}\quad (1)$$

In those expressions, $\hat{\lambda}_\psi$, λ_ϕ and $\hat{\lambda}_\psi$ stand for real coupling strengths, that together with the dark matter (M_S , M_χ and M_V) and mediator (M_ψ , M_ϕ and M_ψ) masses lead to three free parameters for each of the considered models. We collectively denote this set of free parameters by $\{m_X, m_Y, \lambda\}$.

In this work, we allow the two masses m_X and m_Y to vary in the $[1, 10^4]$ GeV range and consider λ coupling values in the $[10^{-4}, 4\pi]$ range (couplings larger than 4π are shown in our results, but the 4π contour is always highlighted when relevant). We use the corresponding next-to-leading-order (NLO) UFO [6] model files with five massless quarks for collider studies with MG5_AMC [7], and both the leading-order (LO) UFO and CALCHEP [8] model files with six massive quarks for simulations with MADDM [9] and MICROMEGAS [10] respectively. All those model files have been obtained with FEYNRULES [11] and are available from <https://feynrules.irmp.ucl.ac.be/wiki/DMSimpt>.

3. Collider bounds

Three types of processes are considered for the determination of the collider constraints on the models. They consist in the production of a pair of dark matter particles ($pp \rightarrow XX$), of a pair of mediators ($pp \rightarrow YY$) and the associate production of a dark matter and a mediator ($pp \rightarrow XY$). Mediator pair-production is itself composed of three components, namely a QCD contribution, a dark-matter-induced contribution (with the propagation of the dark matter particle in the t -channel) and their interference. When the mediator is produced, it subsequently decays into a dark matter candidate and a right-handed up-quark ($Y \rightarrow Xu_R$), the decay process being always factorised from the production one. This however assumes that the decay width of the mediator Γ_Y is small relatively to its mass, such that the narrow-

width approximation (NWA) holds¹. The relative contributions of the different channels depend on the exact details of the model, and in particular on the λ coupling value. In particular, the relevance of the XX channel originates from the emission of jets by the initial state and the internal mediator, that are both considered at the matrix-element and parton-shower level in our NLO simulations matched with parton showers. In terms of the kinematics, the channels with the largest cross section are, however, not necessarily the relevant ones in terms of probing the model parameter space and setting limits, as already illustrated in ref. [5].

All simulations are performed with MG5_AMC and follow the procedure described in ref. [5], the NLO matrix elements being convoluted with the NNPDF 3.0 set of parton densities [13] through the LHAPDF 6 library [14]. Moreover, to ensure the validity of the NWA and the factorisation of the production and decay processes, all simulations have been performed at a fixed Γ_Y/m_Y ratio of 1%, assuming that the final-state kinematics is not impacted by slightly larger values of this ratio. In the following, we reweigh those generated events so that the cross section evaluation makes use of a λ value yielding $\Gamma_Y/m_Y = 5\%$. This choice requires a more important coupling and leads to weaker cosmological constraints, which thus allows for a larger cosmologically-viable region of the parameter space to be probed by LHC searches (see section 4 and section 5). Different choices of the Γ_Y/m_Y ratio can impact the results, as lower Γ_Y/m_Y values imply lower couplings. Besides an expected strengthening of the relic density constraints yielded by a smaller annihilation cross section, it would reduce the relative weights of the XX , XY and non-QCD YY collider channels with respect to QCD YY production whose cross section is independent of λ . On the other hand, larger width-over-mass ratios would make the collider analysis less accurate, as for large widths the NWA-motivated factorisation of the production and decay processes would not accurately describe the kinematics of the final state.

We obtain constraints on the models through the recast of an ATLAS search targeting final states with multiple jets and missing transverse energy [15] by means of the MADANALYSIS 5 framework [16, 17]. This search is well suited to probe scenarios where dark matter interacts with light quark flavours, as considered in this work. While monojet searches could be relevant too, they consist strictly speaking in multi-jet plus missing energy searches, as a subleading jet activity is allowed. They are thus only different from the considered search by the details of the requirements on the event hadronic activity. As no ATLAS and CMS monojet search has been updated as a full run 2 analysis yet, monojet probes will be ignored. Other searches could nevertheless be better in other contexts. For instance, for setups involving interactions with top quarks, searches involving final-state top quarks and missing transverse energy could probably give

¹In principle, the NWA approximation is valid only if the mass difference between the decaying particle and the decay products is large [12]. We however assume that corrections arising from small mass splittings are not significant in the corresponding regions of the parameter space.

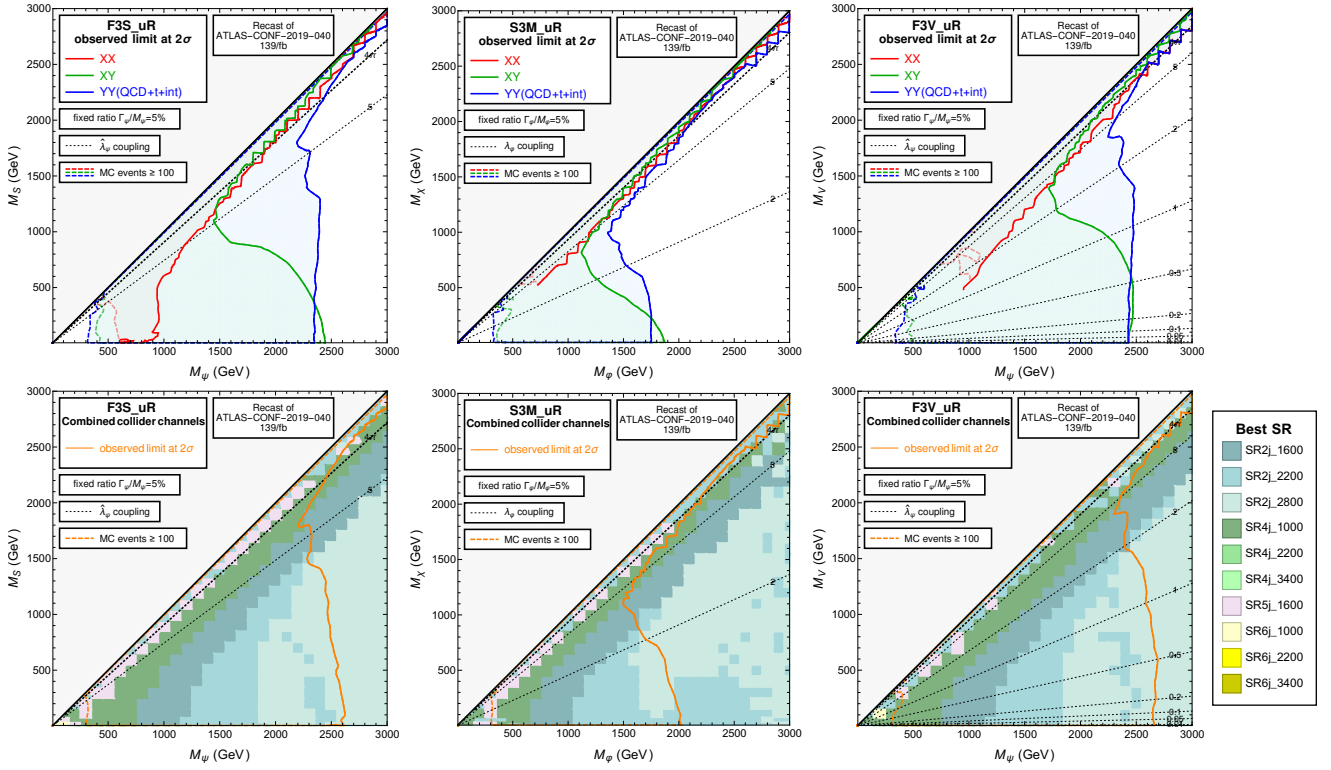


Figure 1: **Top row:** Individual 95% CL bounds arising from the three different channels XX (red), XY (green) and YY (blue) for the F3S_uR (left), S3M_uR (centre) and F3V_uR (right) scenarios, presented in the (m_χ, m_ψ) plane for a fixed mediator width-to-mass ratio. **Bottom row:** Combined 95% CL bounds, with the signal region exhibiting the best sensitivity depicted by the background colour. In all panels, the black dashed lines correspond to the value of the couplings which is required to obtain a width over mass ratio of 5%, the 4π value being highlighted to roughly identify the perturbative regime. The coloured dashed lines identify the area for which the number of simulated Monte Carlo events populating the best region is larger than 100 (allowing for a Poisson uncertainty smaller than 10%).

a slightly better reach, as already found out for instance for scalar [18] or Majorana [19] dark matter. The significance of the signal is derived for each of the ten signal regions (SRs) of the search through the CLs method [20], and we include in our predictions signal systematics stemming from scale variations and the parton density fits [21]. The yields of the backgrounds for each SR, with their uncertainties, and the number of observed events, are provided by the ATLAS search. As observations are compatible with the background within 1σ for all signal regions of relevance, observed and expected bounds do not significantly differ. We show the former in our results. Obviously, for high-luminosity projections (see section 5), expected limits are used for the extrapolations.

Due to the different dependence of the cross sections on the λ coupling and on the masses of the new particles, the relative weights of the XX , XY and YY contributions in the determination of the constraints change along the parameter space, as shown in the top row of fig. 1. The combination of the various contributions to the YY process constrains the majority of the parameter space for all the considered scenarios. In contrast, the XX process only becomes competitive in the compressed region and for large mediator masses, while the XY one provides instead stronger con-

straints for scenarios featuring a large mass gap and a large mediator mass. The region with small dark matter and mediator masses is likely to be excluded too, but the number of initial MC events required to test the region with enough statistics is too demanding in terms of computing resources.

The combination of the bounds for any given scenario is obtained in two steps. We first sum the number of events populating each signal region as obtained from the individual XX , XY and YY contributions, and then compute the corresponding significance. We display the results in the bottom row of fig. 1, in which we additionally highlight the best signal region driving the bound. The dominance of the YY component in the determination of the bounds is reflected in the similarities of the results for the F3S_uR and F3V_uR models that share the same mediator particle. For the S3M_uR class of scenarios, the bounds are sizeably weaker, given the smaller cross section for the pair production of a scalar mediator that features a smaller number of degrees of freedom than a fermion.

The combined signal kinematics for any given scenario depends on the subprocess that dominates, which is reflected in the variations in the best SRs driving the bounds along the parameter space. Regions requiring two very hard jets are more suitable when the YY channel dominates and each

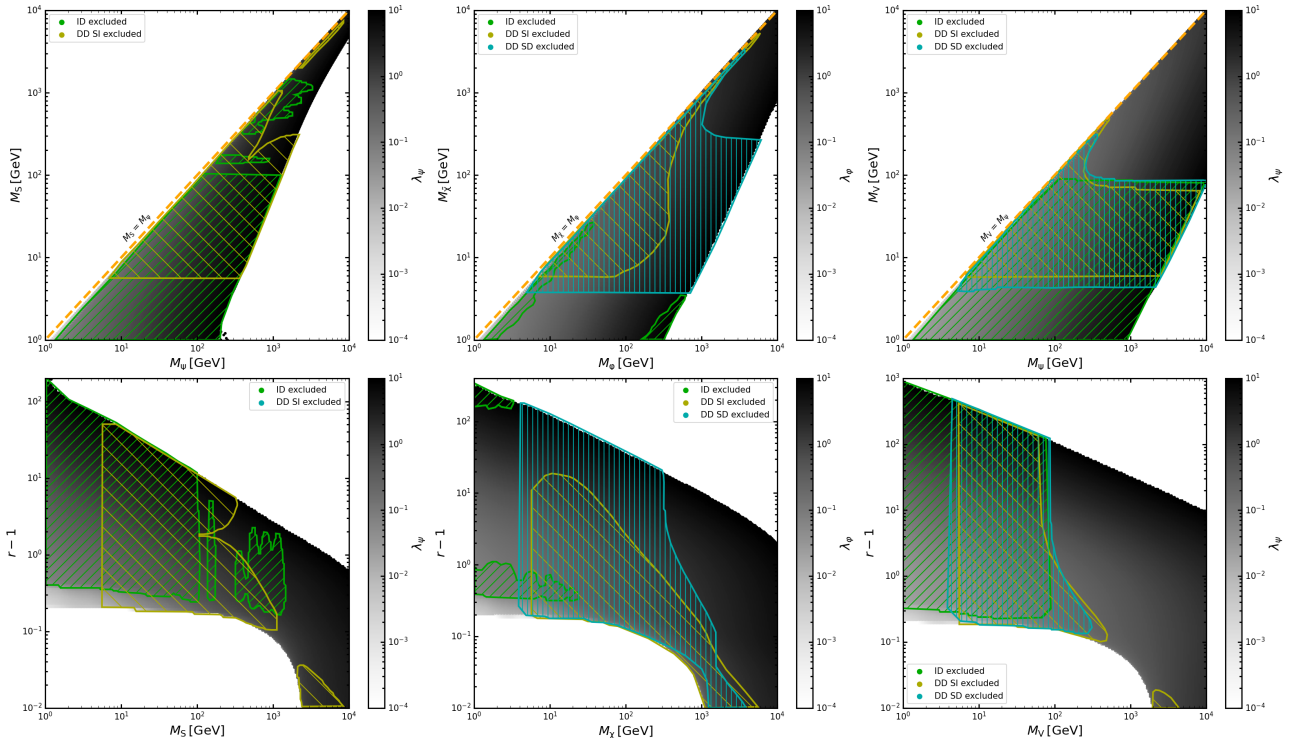


Figure 2: **Top row:** Parameter space regions compatible with the standard freeze-out mechanism and the observed relic density [22], shown in the (m_Y, m_X) plane for the F3S_uR (left), S3M_uR (centre) and F3V_uR (right) models. The gray shading indicates the λ value needed to satisfy the relic density constraint. The yellow hatched region is excluded by the SI XENON1T bounds [23] (DD SI), the green hatched one by gamma-ray line searches from Fermi-LAT [24] and HESS [25] (ID), and the cyan hatched one by the SD PICO bounds [26] (DD SD). Moreover, for the F3V_uR model, indirect detection bounds are extracted from Fermi-LAT in dSphs searches [27] (ID), when one relies on dark matter annihilations in the $u\bar{u}$ final state [9]. **Bottom row:** Same as for the top row but in the $(r-1, m_X)$ plane where $r \equiv m_Y/m_X$. This allows us to highlight better the co-annihilation regime.

mediator decay leads to a significantly hard jet. In contrast, SRs dedicated to final states featuring four jets give a better outcome in the compressed regime. While these regions select events exhibiting a larger number of jets, the associated transverse momentum requirements are milder than in the two-jet case, and thus more efficient in more compressed setups in which decay and radiation jets are softer.

4. Cosmological bounds

For all three models, we sample the three-dimensional parameter space with MICROMEGAS and require that the dark matter candidate makes up 100% of the measured dark matter abundance, $\Omega h_{\text{Planck}}^2 = 0.12$ [22]. The thermally averaged dark matter annihilation cross section $\langle\sigma v\rangle$ (v being the relative velocity between two dark matter particles) is d -wave-suppressed for the real scalar case [28, 29, 30, 31, 32] and p -wave-suppressed for Majorana dark matter [30, 33]. NLO corrections in the relic density computation might therefore be relevant [31, 18]. To account for these corrections, we include the loop-induced $XX \rightarrow gg$ and $XX \rightarrow \gamma\gamma$ processes², and the three-body $XX \rightarrow u_R \bar{u}_R g$ and $XX \rightarrow u_R \bar{u}_R \gamma$ annihilations that could be potentially enhanced by

² $XX \rightarrow \gamma Z$ annihilations should be included as well, as the associated matrix element is of the same perturbative order as the $XX \rightarrow \gamma\gamma$ one. However, we have found out that the di-photon contribution to $\langle\sigma v\rangle$ is

virtual internal bremsstrahlung (VIB). For our predictions, we use the analytic expressions provided in refs. [29, 30, 34] that we have validated with MADDM. While different choices of dark matter interactions (in terms of the flavour and chirality of the involved SM quarks) would lead to a different interplay between the subprocesses contributing to the relic density, it will always be possible to find viable solutions for the λ parameter.

Through our scans of the model parameter spaces, we single out regions where the elastic dark matter scattering cross section off protons is compatible with both the spin-independent (SI) and spin-dependent (SD) exclusion limits at 90% confidence level (CL) from the XENON1T [23] and PICO [26] experiments, our predictions relying on NLO cross sections [35] to properly model the impact of QCD radiation. In principle, running coupling effect should also be included [36]. The latter would lead to tighter exclusion limits, slightly augmenting their sensitivity for large dark matter masses. We have however omitted them from our computations, although we have verified that they do not impact our conclusions. We do not expect the obtained direct detection bounds to sensibly change for different choices of

subdominant to the $XX \rightarrow gg$ one in the entire parameter space. We have therefore not accounted for annihilations into a γZ system, that is itself subleading with respect to $XX \rightarrow \gamma\gamma$.

dark matter interactions with right-handed valence quarks. For other scenarios involving sea quarks, we however expect those bounds to be weakened. Finally, we impose in our scanning procedure that predicted indirect detection signals are compatible with the current (model-dependent) exclusion limits at 95% CL. This time, different choices of dark matter interactions would result in a different weighting of the subprocesses contributing to the gamma-ray signals, and therefore of different results.

In the case of the F3S_uR and S3M_uR models, spectral features in the gamma ray spectrum bring one of the strongest bounds as tree-level $XX \rightarrow u_R \bar{u}_R$ annihilations are velocity suppressed. We therefore derive constraints by considering a combination of direct annihilations into photons and into a $u_R \bar{u}_R \gamma$ system, the latter being potentially enhanced by VIB contributions. The total annihilation cross section $\langle \sigma v \rangle_{\text{tot}} = \langle \sigma v \rangle_{u_R \bar{u}_R \gamma} + 2\langle \sigma v \rangle_{\gamma\gamma}$ is then confronted with the most recent Fermi-LAT [24] and HESS [25] data from the Galactic Centre³. We assume that the gamma-ray spectrum related to the $u_R \bar{u}_R \gamma$ contribution presents a sharp feature close to the dark matter mass, even though the exact position of this feature depends on $r \equiv m_Y/m_X$ [38]. The obtained constraints are in the worst case conservative, although for most scanned over scenarios they consist in a good approximation. The three-body signal indeed dominates over the di-photon one, at least at small r values, so that the peak is often very close to the dark matter mass. The derivation of more precise constraints would require a recast of the experimental results, which lies beyond the scope of this study.

Other relevant bounds can be obtained by investigating dark matter annihilations into gluons, as this could be constrained by the Fermi-LAT analysis of dwarf spheroidal galaxies (dSphs) data [27]. Similarly to the gamma-ray case, we evaluate $\langle \sigma v \rangle_{\text{tot}} = \langle \sigma v \rangle_{u_R \bar{u}_R g} + \langle \sigma v \rangle_{gg}$ and compare our predictions with Fermi-LAT dSph results for the gg annihilation channel [9]. These constraints being comparable with those arising from gamma-ray line searches, they are omitted from the discussion. Finally for the F3V_uR model, $XX \rightarrow u_R \bar{u}_R$ annihilations occur in an s -wave configuration. The most stringent indirect detection bounds are thus given by Fermi-LAT dSph searches, this time in the $u\bar{u}$ final state.

Our results are shown in fig. 2. The gray shaded region represents scenarios that can account for the correct relic density when assuming a standard freeze-out mechanism. For the F3S_uR model, NLO corrections drastically modify the contours of the viable parameter space region at large r , selecting λ values smaller than for the LO case. This stems from the $XX \rightarrow gg$ contributions, that are driven by the strong coupling constant α_s and that enhance the annihilation cross section. On the contrary, NLO corrections for the Majorana dark matter case do not impact the results much. In the large r regime, we obtain deviations in the λ value of at most 15% with respect to the LO case, whilst scenarios featuring a small r value are unaffected, the annihilation cross section being dominated by α_s -dependent co-annihilations.

Following the same reasoning, it turns out that the actual value of λ is irrelevant when co-annihilations of the mediator via QCD processes drive the relic density.

The F3V_uR model is the one that features the largest parameter space for which the relic density as measured by the Planck collaboration can be accommodated. For any given (m_X, m_Y) mass configuration, the λ value that is needed to obtain $\Omega h^2_{\text{Planck}}$ is smaller than in the scalar and Majorana dark matter cases. The annihilation strength of vector dark matter is indeed larger, except in the co-annihilation regime where the model is indistinguishable from the F3S_uR setup that also features a fermionic mediator.

Our findings show a nice complementarity between direct and indirect dark matter searches in the case of the F3S_uR and F3V_uR models. Gamma-ray searches (green hatched region) are able to probe and disfavour at 95% CL dark matter candidates with masses ranging down to 1 GeV, except for compressed spectra with $r - 1 \lesssim 0.3$ and very small couplings below about 10^{-2} (bottom row of fig. 2). This unexplored region consists in one of the two co-annihilation-dominated regions which are still open and might give rise to interesting LHC signatures through long lived particles (LLPs) [39]. For the S3M_uR model, indirect detection plays a minor role, excluding a limited part of the parameter space where dark matter is light. The two separated excluded regions correspond to Fermi-LAT limits arising from $XX \rightarrow \gamma\gamma$ (large r values) and $XX \rightarrow u_R \bar{u}_R \gamma$ (small r values) annihilations respectively. Finally, F3S_uR scenarios can be proved by the HESS experiment, as depicted by the disfavoured island in the parameter space at $m_X > 300$ GeV.

Direct and indirect detection bounds both exclude the intermediate mass range, although direct detection bounds additionally contribute to cut down the parameter space. This is particularly true for large dark matter masses, close to 1 TeV or even higher, where one finds a second viable co-annihilation regime and where the XENON1T bounds (yellow hatched region) start to play a role. In addition, very light dark matter scenarios are excluded due to PICO constraints (cyan hatched region). Remarkably, these two direct detection experiments are also able to probe the co-annihilation regime. The whole freeze out parameter space is hence disfavoured at 90% CL for dark matter masses between 4 GeV and 1000 (500) GeV for the F3S_uR (F3V_uR) model.

Spin-dependent direction detection exclusion bounds are the most stringent constraints on the S3M_uR model parameter space, even though spin-independent experiments start to be sensitive to dark matter masses larger than 4 TeV. Majorana dark matter is strongly disfavoured for masses between 8 and 300 GeV, even for the co-annihilation regime that could give rise to LLP collider signatures. The latter regime is even further constrained, for dark matter masses ranging up to 10 TeV, by the XENON1T SI bounds, these constraints being due to the scalar nature of the mediator.

³We derive exclusion limits by considering an Einasto dark matter density profile [37].

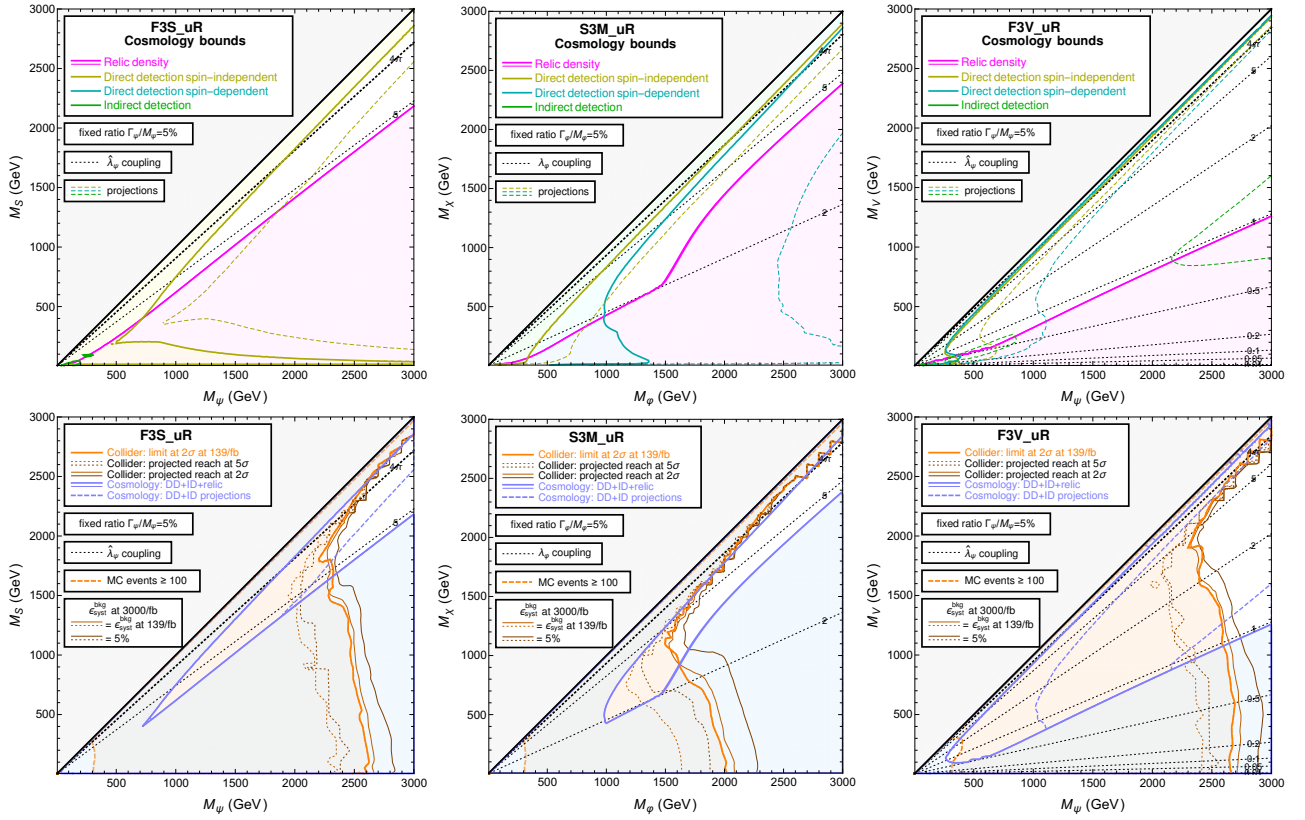


Figure 3: **Top row:** Bounds arising from cosmological observations, represented in the (m_χ, m_γ) plane for a fixed mediator width over mass ratio of 5%, on the F3S_uR (left), S3M_uR (centre) and F3V_uR (right) model parameter space. We allow for under-abundant dark matter, the band which reproduces the relic density as measured by the Planck collaboration lying between the (almost indistinguishable) thin and thick magenta lines. Future projections of the constraints are provided as dashed lines. **Bottom row:** Combination of cosmological and collider bounds and their projections. The collider projections correspond to exclusion and discovery reaches for a LHC luminosity of 3000 fb^{-1} (i.e. the HL-LHC phase) and assume a level of systematics on the background either equal to the considered ATLAS search at current luminosity or fixed to 5%.

5. Combining dark matter searches

We illustrate in fig. 3 the complementarity of the considered cosmological and collider constraints on the models, after mapping the cosmological bounds of section 4 onto an (m_χ, m_γ) plane for a fixed Γ_Y/m_Y ratio of 5%⁴. However, contrary to the previous section, we allow for under-abundant dark matter and therefore only consider the relic density constraint as an upper bound. We hence implicitly assume the existence of some other dark matter component, with different properties and interactions.

Under these assumptions, we obtain allowed parameter space regions for all scenarios. These regions feature mediator masses greater than 1.5 TeV (scalar mediator) and 2 TeV (fermion mediator), and a neither too compressed nor too split new physics spectrum. The mediator mass is mostly constrained by collider searches, while the dark matter mass

⁴Representing the results for a fixed mediator width-over-mass ratio is only one of the possibilities. We could instead enforce a fixed λ value. In this case, Γ_Y/m_Y increases for large mediator and small dark matter masses. The NWA can thus break down, depending on the value of the coupling and on the model, and simulations relying on the factorisation of the mediator production and decay processes, as traditionally performed, would lead to an incorrect description of the signal kinematics.

is restricted by the combination of the relic density (lower bound) and the interplay between the SD and SI direct detection (upper bound) constraints. The only exception concerns the small mass gap regime in which the collider constraints tend to be competitive (despite of potentially non-perturbative couplings). For all scenarios, indirect detection constraints are too weak to play any role. Gamma-ray fluxes are indeed reduced by a $(\Omega h^2_{\text{model}}/\Omega h^2_{\text{Planck}})^2$ factor for under-abundant dark matter, contrarily to the direct detection predictions that are only linearly rescaled⁵.

This collider-cosmology complementarity of constraints is compatible with the nature of the considered experimental probes. Collider bounds are largely dominated by the impact of the YY channel. On the contrary, direct detection experiments are more sensitive to scenarios featuring large couplings and/or a small X/Y mass splitting, as the direct detection cross section scales as λ^4 and exhibits a polynomial in r in its denominator. Moreover, when allowing for

⁵Without such a rescaling (as when a non-thermal mechanism is invoked to reproduce the dark matter density [40]), the combination of current direct and indirect detection bounds disfavors the parameter space regions which the HL-LHC is sensitive to. We do not consider such a possibility in this work.

under-abundant dark matter, the relic density favours large couplings as well and opens the door to a much wider set of viable solutions.

In the same fig. 3, we provide projections for future experiments. We show projected 2σ exclusion and 5σ discovery reaches for the HL-LHC, which corresponds to a luminosity of 3 ab^{-1} . We extrapolate the current reach under two assumptions for the manner the systematic uncertainties on the background $\epsilon_{\text{syst}}^{\text{bgk}}$ could evolve. In a first case, we consider that it is the same as in the initially considered 139 fb^{-1} ATLAS search, while in the second case, we assume that it reaches a floor of 5% for each SR. The results show that considering the recast cut-and-count ATLAS analysis, the bounds will not improve significantly even with an optimistic assumption on the systematics. Equivalently, this shows that the discovery reach is very close to the current exclusion limits. Different, more complex, analysis strategies should therefore be considered to better assess the potential of future searches in probing a wider region of the parameter space. For example, the ATLAS search that we have used in our analysis also includes a supersymmetry-inspired signal region relying on a boosted decision tree, which we did not consider in our model-independent approach.

On the other hand, the projected cosmological bounds have a much larger potential. We present the expected sensitivity of future SI (LZ [41]) and SD (LZ, PICO-500 [42] and COSINUS [43]) direct detection experiments, the latter being extracted from ref. [44] for the \mathcal{O}_4 operator (*i.e.* for standard SD interactions). The interplay of the projected SD bounds and the relic density constraints can completely exclude the S3M_{uR} scenario, while the improvement of the SI bounds would drastically limit the options allowed by the HL-LHC expectation for the F3S_{uR} model. Similarly, high-energy gamma-ray experiments, such as CTA [45, 46] and SWGO [47], and the LSST+Fermi-LAT dSphs survey [48] will be able to explore the model parameter space well above the TeV regime, in a region that is out of reach of LHC searches. In particular, projections for indirect detection has the largest impact on the F3V_{uR} scenario, being the dominant constraint for large mediator masses. It however still leaves a large window testable at the HL-LHC.

6. Conclusions

We have performed a comprehensive analysis of cosmological and collider bounds for three sets of t -channel simplified dark matter models in which the dark matter is a real field. We have investigated the complementarity between the different types of bounds and made projections for future collider and cosmological experiments. Our findings show that most parameter spaces are already strongly constrained by current bounds, and that future dark matter direct and indirect detection probe have a large potential to cover the still allowed regions of the parameter space. In this way, conclusive statements on the phenomenological viability of the considered class of t -channel models will be in order in the next decades.

One should however keep in mind that the models considered in this analysis are simplified and model-independent constructions. While being representative of different theoretically-motivated new physics scenarios, they necessarily lack non-minimal features, such as the presence of more mediators, a multi-component dark matter spectrum, or a wider range of interactions between the new particles and the SM. Such features can change the picture by introducing, for example, interference contributions which can weaken the constraints or effects due to large mediator widths which modify the final-state kinematics at colliders.

Finally, we did not investigate freeze-in dark matter scenarios, which we leave for a separate work. This scenario is viable for tiny λ values of the order of 10^{-6} or smaller and might open up additional windows, as for instance related to LLP searches at the LHC.

Acknowledgments

We acknowledge J. Heisig, M. Kraemer and K. Mawatari for stimulating discussions during this study, and L. Lopez Honorez and M. Tytgat for their help in the validation procedure. LP work is supported by the Knut and Alice Wallenberg foundation under the SHIFT project, grant KAW 2017.0100. LP acknowledges the use of the IRIDIS 4 HPC Facility at the University of Southampton. CA is supported by the Innoviris ATTRACT 2018 104 BECAP 2 agreement. HM is supported by the German Research Foundation DFG through the RTG 2497 and the CRC/Transregio 257. LM is supported by funding from the European Union's Horizon 2020 research and innovation programme as part of the Marie Skłodowska-Curie Innovative Training Network MC-netITN3 (grant agreement no. 722104).

References

- [1] J. Silk et al., *Particle Dark Matter: Observations, Models and Searches*. Cambridge Univ. Press, Cambridge, 2010, [10.1017/CBO9780511770739](https://doi.org/10.1017/CBO9780511770739).
- [2] P. J. Fox and C. Williams, *Next-to-Leading Order Predictions for Dark Matter Production at Hadron Colliders*, *Phys. Rev. D* **87** (2013) 054030 [[1211.6398](https://arxiv.org/abs/1211.6398)].
- [3] U. Haisch, F. Kahlhoefer and E. Re, *QCD effects in mono-jet searches for dark matter*, *JHEP* **12** (2013) 007 [[1310.4491](https://arxiv.org/abs/1310.4491)].
- [4] M. Backovic, M. Kraemer, F. Maltoni, A. Martini, K. Mawatari and M. Pellen, *Higher-order QCD predictions for dark matter production at the LHC in simplified models with s-channel mediators*, *Eur. Phys. J. C* **75** (2015) 482 [[1508.05327](https://arxiv.org/abs/1508.05327)].
- [5] C. Arina, B. Fuks and L. Mantani, *A universal framework for t-channel dark matter models*, *Eur. Phys. J. C* **80** (2020) 409 [[2001.05024](https://arxiv.org/abs/2001.05024)].
- [6] C. Degrande, C. Duhr, B. Fuks, D. Grellscheid, O. Mattelaer and T. Reiter, *UFO - The Universal FeynRules Output*, *Comput. Phys. Commun.* **183** (2012) 1201 [[1108.2040](https://arxiv.org/abs/1108.2040)].
- [7] J. Alwall, R. Frederix, S. Frixione, V. Hirschi, F. Maltoni, O. Mattelaer et al., *The automated computation of tree-level and next-to-leading order differential cross sections, and their matching to parton shower simulations*, *JHEP* **07** (2014) 079 [[1405.0301](https://arxiv.org/abs/1405.0301)].
- [8] A. Belyaev, N. D. Christensen and A. Pukhov, *CalcHEP 3.4 for collider physics within and beyond the Standard Model*, *Comput. Phys. Commun.* **184** (2013) 1729 [[1207.6082](https://arxiv.org/abs/1207.6082)].

- [9] F. Ambrogio et al., *MadDM v.3.0: a Comprehensive Tool for Dark Matter Studies*, *Phys. Dark Univ.* **24** (2019) 100249 [[1804.00044](#)].
- [10] G. Belanger, F. Boudjema, A. Goudelis, A. Pukhov and B. Zaldivar, *micrOMEGAs5.0: Freeze-in*, *Comput. Phys. Commun.* **231** (2018) 173 [[1801.03509](#)].
- [11] A. Alloul, N. D. Christensen, C. Degrande, C. Duhr and B. Fuks, *FeynRules 2.0 - A complete toolbox for tree-level phenomenology*, *Comput. Phys. Commun.* **185** (2014) 2250 [[1310.1921](#)].
- [12] D. Berdine, N. Kauer and D. Rainwater, *Breakdown of the Narrow Width Approximation for New Physics*, *Phys. Rev. Lett.* **99** (2007) 111601 [[hep-ph/0703058](#)].
- [13] NNPDF collaboration, *Parton distributions for the LHC Run II*, *JHEP* **04** (2015) 040 [[1410.8849](#)].
- [14] A. Buckley, J. Ferrando, S. Lloyd, K. Nordström, B. Page, M. Rüfenacht et al., *LHAPDF6: parton density access in the LHC precision era*, *Eur. Phys. J. C* **75** (2015) 132 [[1412.7426](#)].
- [15] ATLAS collaboration, *Search for squarks and gluinos in final states with jets and missing transverse momentum using 139 fb⁻¹ of $\sqrt{s} = 13$ TeV pp collision data with the ATLAS detector*, ATLAS-CONF-2019-040.
- [16] E. Conte and B. Fuks, *Confronting new physics theories to LHC data with MADANALYSIS 5*, *Int. J. Mod. Phys. A* **33** (2018) 1830027 [[1808.00480](#)].
- [17] F. Ambrogio, *MadAnalysis 5 recast of ATLAS-CONF-2019-040*, 2019. DOI: 10.7484/INSPIREHEP.DATA.45EF.23SB.
- [18] S. Colucci, B. Fuks, F. Giacchino, L. Lopez Honorez, M. H. G. Tytgat and J. Vandecasteele, *Top-philic Vector-Like Portal to Scalar Dark Matter*, *Phys. Rev. D* **98** (2018) 035002 [[1804.05068](#)].
- [19] M. Garny, J. Heisig, M. Hufnagel and B. Luelf, *Top-philic dark matter within and beyond the WIMP paradigm*, *Phys. Rev. D* **97** (2018) 075002 [[1802.00814](#)].
- [20] A. L. Read, *Presentation of search results: The CL(s) technique*, *J. Phys. G* **28** (2002) 2693.
- [21] J. Y. Araz, M. Frank and B. Fuks, *Reinterpreting the results of the LHC with MadAnalysis 5: uncertainties and higher-luminosity estimates*, *Eur. Phys. J. C* **80** (2020) 531 [[1910.11418](#)].
- [22] PLANCK collaboration, *Planck 2018 results. VI. Cosmological parameters*, *Astron. Astrophys.* **641** (2020) A6 [[1807.06209](#)].
- [23] XENON collaboration, *Dark Matter Search Results from a One Ton-Year Exposure of XENONIT*, *Phys. Rev. Lett.* **121** (2018) 111302 [[1805.12562](#)].
- [24] FERMI-LAT collaboration, *Updated search for spectral lines from Galactic dark matter interactions with pass 8 data from the Fermi Large Area Telescope*, *Phys. Rev. D* **91** (2015) 122002 [[1506.00013](#)].
- [25] HESS collaboration, *Search for γ -Ray Line Signals from Dark Matter Annihilations in the Inner Galactic Halo from 10 Years of Observations with H.E.S.S.*, *Phys. Rev. Lett.* **120** (2018) 201101 [[1805.05741](#)].
- [26] PICO collaboration, *Dark Matter Search Results from the PICO-60 C₃F₈ Bubble Chamber*, *Phys. Rev. Lett.* **118** (2017) 251301 [[1702.07666](#)].
- [27] DES, FERMI-LAT collaboration, *Searching for Dark Matter Annihilation in Recently Discovered Milky Way Satellites with Fermi-LAT*, *Astrophys. J.* **834** (2017) 110 [[1611.03184](#)].
- [28] T. Toma, *Internal Bremsstrahlung Signature of Real Scalar Dark Matter and Consistency with Thermal Relic Density*, *Phys. Rev. Lett.* **111** (2013) 091301 [[1307.6181](#)].
- [29] F. Giacchino, L. Lopez-Honorez and M. H. G. Tytgat, *Scalar Dark Matter Models with Significant Internal Bremsstrahlung*, *JCAP* **1310** (2013) 025 [[1307.6480](#)].
- [30] F. Giacchino, L. Lopez-Honorez and M. H. G. Tytgat, *Bremsstrahlung and Gamma Ray Lines in 3 Scenarios of Dark Matter Annihilation*, *JCAP* **1408** (2014) 046 [[1405.6921](#)].
- [31] F. Giacchino, A. Ibarra, L. Lopez Honorez, M. H. G. Tytgat and S. Wild, *Signatures from Scalar Dark Matter with a Vector-like Quark Mediator*, *JCAP* **1602** (2016) 002 [[1511.04452](#)].
- [32] S. Biondini and S. Vogl, *Scalar dark matter coannihilating with a coloured fermion*, *JHEP* **11** (2019) 147 [[1907.05766](#)].
- [33] S. Biondini and S. Vogl, *Coloured coannihilations: Dark matter phenomenology meets non-relativistic EFTs*, *JHEP* **02** (2019) 016 [[1811.02581](#)].
- [34] A. Ibarra, T. Toma, M. Totzauer and S. Wild, *Sharp Gamma-ray Spectral Features from Scalar Dark Matter Annihilations*, *Phys. Rev. D* **90** (2014) 043526 [[1405.6917](#)].
- [35] J. Hisano, R. Nagai and N. Nagata, *Effective Theories for Dark Matter Nucleon Scattering*, *JHEP* **05** (2015) 037 [[1502.02244](#)].
- [36] K. A. Mohan, D. Sengupta, T. M. P. Tait, B. Yan and C. P. Yuan, *Direct Detection and LHC constraints on a t -Channel Simplified Model of Majorana Dark Matter at One Loop*, *JHEP* **05** (2019) 115 [[1903.05650](#)].
- [37] J. Einasto, *Dark Matter*, in *Astronomy and Astrophysics 2010*, [Eds. Oddbjørn Engvold, Rolf Stabell, Bożena Czerny, John Lattanzio], in *Encyclopedia of Life Support Systems (EOLSS)*, Developed under the Auspices of the UNESCO, Eolss Publishers, Oxford, UK, 2009, 0901.0632.
- [38] M. Garny, A. Ibarra, M. Pato and S. Vogl, *Internal bremsstrahlung signatures in light of direct dark matter searches*, *JCAP* **1312** (2013) 046 [[1306.6342](#)].
- [39] J. Alimena et al., *Searching for Long-Lived Particles beyond the Standard Model at the Large Hadron Collider*, *J. Phys. G* **47** (2020) 090501 [[1903.04497](#)].
- [40] R. Allahverdi, B. Dutta and K. Sinha, *Non-thermal Higgsino Dark Matter: Cosmological Motivations and Implications for a 125 GeV Higgs*, *Phys. Rev. D* **86** (2012) 095016 [[1208.0115](#)].
- [41] B. Mount et al., *LUX-ZEPLIN (LZ) Technical Design Report*, 1703.09144.
- [42] PICO collaboration, *Improved dark matter search results from PICO-2L Run 2*, *Phys. Rev. D* **93** (2016) 061101 [[1601.03729](#)].
- [43] G. Angloher et al., *The COSINUS project - perspectives of a NaI scintillating calorimeter for dark matter search*, *Eur. Phys. J. C* **76** (2016) 441 [[1603.02214](#)].
- [44] S. Kang, S. Scopel, G. Tomar and J.-H. Yoon, *Present and projected sensitivities of Dark Matter direct detection experiments to effective WIMP-nucleus couplings*, *Astropart. Phys.* **109** (2019) 50 [[1805.06113](#)].
- [45] V. Lefranc, E. Moulin, P. Panci, F. Sala and J. Silk, *Dark Matter in γ lines: Galactic Center vs dwarf galaxies*, *JCAP* **09** (2016) 043 [[1608.00786](#)].
- [46] CTA collaboration, *Pre-construction estimates of the Cherenkov Telescope Array sensitivity to a dark matter signal from the Galactic centre*, 2007.16129.
- [47] A. Viana, H. Schoorlemmer, A. Albert, V. de Souza, J. P. Harding and J. Hinton, *Searching for Dark Matter in the Galactic Halo with a Wide Field of View TeV Gamma-ray Observatory in the Southern Hemisphere*, *JCAP* **12** (2019) 061 [[1906.03353](#)].
- [48] LSST DARK MATTER GROUP collaboration, *Probing the Fundamental Nature of Dark Matter with the Large Synoptic Survey Telescope*, 1902.01055.